Control by ATR-FTIR of surface treatment of cork stoppers and its effect on their mechanical performance

Jose R. Gonzalez-Adrados, Maria C. Garcia-Vallejo, Maria J. Caceres-Esteban, Jose L. Garcia de Ceca, Florentino Gonzalez-Hernandez, et al.

Online First
Immediately Online
springerlink.com
Faster publication!

Springer

Springer

ORIGINAL

Control by ATR-FTIR of surface treatment of cork stoppers and its effect on their mechanical performance

**Jose R. Gonzalez-Adrados · Maria C. Garcia-Vallejo ·
Maria J. Caceres-Esteban · Jose L. Garcia de Ceca ·
Florentino Gonzalez-Hernandez · Rosa Calvo-Haro**

Abstract   Fourier transform infrared (FTIR) spectroscopy was applied to determine the type of surface treatment and dose used on cork stoppers and to predict the friction between stopper and bottleneck. Agglomerated cork stoppers were finished with two different doses and using two surface treatments: P (paraffin and silicone), 15 and 25 mg/stopper, and S (only silicone), 10 and 15 mg/stopper. FTIR spectra were recorded at five points for each stopper by attenuated total reflectance (ATR). Absorbances at 1,010, 2,916, and 2,963 cm^{-1} were obtained in each spectrum. Discriminant analysis techniques allowed the treatment, and dose applied to each stopper to be identified from the absorbance values. 91.2% success rates were obtained from individual values and 96.0% from the mean values of each stopper. Spectrometric data also allowed treatment homogeneity to be determined on the stopper surface, and a multiple regression model was used to predict the friction index (If = Fe/Fc) ($R^2 = 0.93$).

Introduction

The purpose of the surface treatment of cork stoppers is to coat the stopper with a lubricant film in order to reduce friction, thereby enabling the stopper to be inserted in and extracted from the neck of the bottle with greater ease. The application of this treatment causes a reduction in the dynamic friction index and, correspondingly, in the stopper extraction strength, which has been evaluated at about 30% of their values (Fortes et al. 2004).

J. R. Gonzalez-Adrados (✉) · M. C. Garcia-Vallejo · M. J. Caceres-Esteban ·
J. L. Garcia de Ceca · F. Gonzalez-Hernandez · R. Calvo-Haro
INIA, Ctra. A Coruña km 7.5, 28040 Madrid, Spain
e-mail: adrados@inia.es

Surface treatment also improves the sealing behavior of cork due to the hydrophobic properties of the applied products, usually paraffin and silicone of food grade quality (Pereira 2007). This improvement is due to the decrease in the wettability of the material, altered by the washing processes (Chatonnet and Labadie 2003; Fortes et al. 2004). Thus, the surface treatment decreases the flow of liquid (percolation) between the stoppers and the bottleneck (Gonzalez-Adrados et al. 2008). On the other hand, it may affect the air permeability, which is very important in the process of aging wine in the bottle (Kontoudakis et al. 2008; Lopes et al. 2007; Skouroumounis et al. 2005), one of the most studied aspects in recent years.

Several analysis methods have been proposed to control stopper surface treatments. Qualitative analyses, which are the focus of pollutant detection, have been carried out by extracting the treatment products with solvents and analyzing them by GC–MS (Bradley and Castle 2003). At present, the possibility of sanitary problems related to migration of compounds used in surface treatment has been ruled out (Six and Feigenbaum 2003; Six et al. 2002). Extraction with solvents has been attempted as a complementary method to control the quantity of treatment applied to stoppers, although this did not prove useful, especially for silicones (Riboulet and Alegoët 1986). Other methods habitually used are the measurement of absorption and the static angle of liquid-surface contact (Chatonnet and Labadie 2003). Finally, indirect control of the quality of the treatment can be achieved by measuring the force necessary to extract the stopper, which is a parameter that characterizes the cork's mechanical behavior (Giunchi et al. 2008). None of the methods described provides information on the quantity of treatment product deposited on the surface or the homogeneity of its distribution.

A previous study (Ortega-Fernandez et al. 2006) reported on the possibility of detecting the presence and the type of treatment applied to a stopper by using the attenuated total reflectance-fourier transform infrared (ATR-FTIR) technique. The same technique has been applied recently for the characterization of paper finishes (Canals et al. 2008) and to determine polymeric film thickness from 10 to 110 nm (Yang et al. 2005), thinner than that used to coat cork stoppers.

The objectives of this study are the application of ATR-FTIR techniques to discriminate stoppers treated with different types and doses of surface treatment, as well as to evaluate treatment homogeneity by comparing the spectrum intensity at different points on the stopper. Additionally, the application of this technique to predict stopper behavior in terms of friction is set out.

Materials and methods

Surface treatment products

From the products available in the market, two were selected which were considered representative: the "P" product, a mixture of paraffin, wax, silicone, and aliphatic solvent; and the "S" product, neutral–reticulate elastomeric mixtures of dimethylsiloxane polymers and white pigment.

Samples

Regular agglomerated cork stoppers for bottling wine were used. This type of stopper was selected due to its greater homogeneity and thus minimizing the matrix effect on the spectra.

Five lots of 500 units were extracted randomly from a batch of 10,000 agglomerated stoppers with nominal dimensions of 23×44 mm^2, washed with hydrogen peroxide. One of the lots (product "00") was not treated at all and used as a reference. The selected treatments were applied to the rest of them in an industrial revolving drum, under the conditions specified by the products' supplier (30 min at 20–25 rpm). From each product, two different doses were applied: one 25% larger and the other 25% smaller than that recommended by the manufacturer. Sample characteristics are shown in Table 1.

After treatment, five stoppers for each lot were selected to assure the highest possible homogeneity for density (average density of 0.3035 g cm^{-3}, CV = 2.7%).

Infrared spectroscopy

The FTIR spectrometer was a FTIR460 Plus instrument from Jasco, USA, equipped with a MIRacle ATR accessory from Pike Technologies, USA, with ZnSe lenses and a single-reflection diamond ATR element. The crystal plate assembly of the MIRacle single-reflection ATR features a round plate design, with a diameter of 1.8 mm in the sampling area located in the centre. Resolution was 1 cm^{-1}, and 200 scans were accumulated in order to improve the signal to noise ratio. The contact pressure between clamp and sample was 10,000 psi. Data were collected using the Jasco Spectra Analysis program.

A total of 5 determinations (spectra) were made from the lateral surface of each sample. A total of 125 spectra were analyzed. Baseline correction was applied to all spectra, adjusting the line at 900, 1,800, and 4,000 cm^{-1}. The noise level was set to 0.02. Absorbance numerical values were obtained from each spectrum for the predetermined wavelengths (Ortega-Fernandez et al. 2006).

Extraction with dichloromethane (DCM)

After FTIR analysis, each stopper was processed for extraction with dichloromethane (DCM), in a Soxhlet device (Büchi) for a period of 4 h. After concluding the

Table 1 Sample characteristics: type of surface treatment product and dose applied

Identification	Dose (mg/stopper)	Product
00	0	None
P1	15	Mixture of paraffin, wax, silicone and aliphatic solvent
P2	25	
S1	10	Neutral–reticulate elastomeric mixtures of dimethylsiloxane
S2	15	polymers and white pigment

process, the dry residue per stopper was determined applying the Büchi program for DCM extraction and finished with oven drying at 103°C until constant weight.

Friction measurement

Prior to measuring FTIR and DCM extraction, the bottling process was simulated with each stopper by using a semiautomatic cork capping machine with four clamps. This device is activated by 400-W Panasonic servomotors (for clamp compression and stopper expulsion), which incorporates two load cells of 0.1 N precision (Utilcell 650, 1T, TEASA, Barcelona, Spain). By means of these cells, it was possible: (1) to register the maximum strength needed to compress the stopper to a diameter of 16 mm ($\varepsilon = 33\%$) (Fc) and (2) to register the maximum strength needed to expel the stopper from the clamps (Fe). Friction index (If) is defined as the relation between both forces:

$$If = \frac{Fe}{Fc}$$

Statistical analysis

After preliminary descriptive analysis (means, graphs), univariate (nested-design ANOVA, regression) and multivariate (principal component analysis, stepwise discriminant analysis, and canonical discriminant analysis) analyses were applied to several variables (individual and mean absorbances at selected frequencies, friction index, DCM extract). Multivariate analyses were performed on typified variables. Cross-validation of discriminant functions was done using the jacknife method. Software used was SPSS Statistics 17.0 and GLM, REG, DISCRIM, and CANDIS procedures from SAS Statistical Analysis System, Version 9.

Discussion and results

Determination of surface treatment type and dose by ATR-FTIR

FTIR spectra

The spectra type for each treatment is shown in Fig. 1. Bands at 1,258, 1,079, 1,010, and 787 cm^{-1}, assigned to Si–O bonds, and at 2,963, 2,916, and 2,850 cm^{-1}, corresponding to C–H bonds, are related to silicones and paraffins. The bands of the later group are not specific to paraffin but present very different intensities in both types of compounds. The band at 2,963 cm^{-1}, due to CH3, is much more intense in silicones than in paraffins. In silicones CH3 is almost the only alkyl radical, while in paraffins the principal group is CH2, being CH3 in a much lower proportion. The bands at 2,916 and 2,850 cm^{-1} are due to the methylene groups, which are dominant in paraffins and also in some cork components. Therefore, there may be some overlap between CH2 from paraffins and from underlying cork.
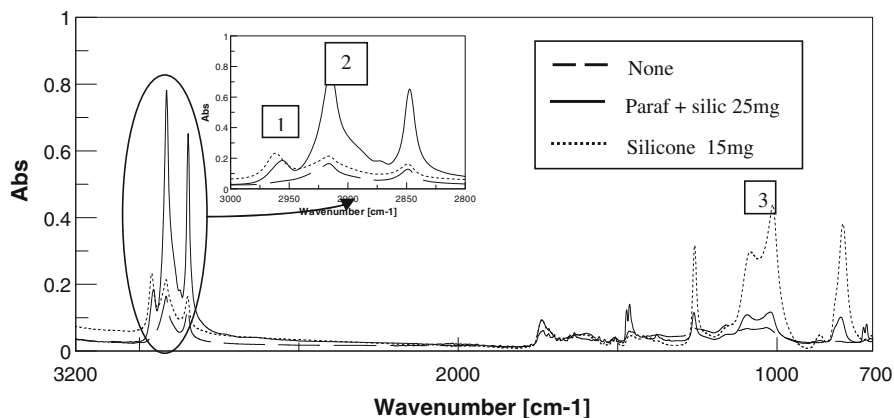
Fig. 1 Spectra obtained from untreated reference (00) and samples with P2 (paraffin and silicone) and S2 (silicone) treatments. Three bands are selected. 1: 2,963 cm^{-1}; 2: 2,916 cm^{-1}; 3: 1,010 cm^{-1}

A principal components analysis was conducted with the absorbance data obtained from each band, showing that two canonical axes absorbed 99% of the variance. The variable with the highest correlation with the first axis is absorbance at 1,010 cm^{-1} and with the second axis, absorbance at 2,916 cm^{-1}. In the rest of the bands, the absorbances show correlations higher than 0.99 with those two bands, except for the band at 2,963 cm^{-1}, where correlation with the silicone bands fluctuates from 0.82 to 0.85.

Based on these results, the statistical analysis was reduced to three absorbance variables: bands at 1,010 cm^{-1} (abs1010), 2,916 cm^{-1} (abs2916), and 2,963 cm^{-1} (abs2963). In addition to the 125 original observations for each variable (5 treatments × 5 stoppers × 5 measures), the mean values of the five measurements taken from each stopper (abs1010av, abs2916av, and abs2963av) were also used.

The spectra also exhibit other bands corresponding to the cork matrix, the most intense occurring at 1,735 cm^{-1} due to carbonyl bonds mainly from suberin, and bands at 1,010–1,300 cm^{-1}, mainly due to carbohydrate and lignin C–O bond. The latter can overlap with those of silicone.

Comparison between DCM extraction and FTIR analysis

Table 2 shows mean values and standard deviations of the extracts in dichloromethane (DCM) and mean absorbances of the three selected IR bands for each treatment and dose. ANOVA results are also included. Absorbance for band at 2,963 cm^{-1} was not measured for the "00" treatment due to the fact that the peak definition was quite imprecise.

None of the factors analyzed (treatment and dose) showed any effect on the DCM extract. This fact discards using this method to determine the treatment amount applied. The reason is that the biggest part of the extract consists of natural cork compounds.

Table 2 Mean values (standard deviation) and ANOVA results for the dry extract in dichloromethane and average absorbances of the selected bands for each stopper

Treatment	DCM dry extract (mg)	abs1010av	abs2916av	abs2963av
00	47.20 (2.94)	0.041 (0.002)	0.151 (0.018)	0.000 (0.000)
$P1$	51.74 (1.85)	0.073 (0.007)	0.416 (0.062)	0.121 (0.014)
$P2$	54.83 (3.49)	0.087 (0.031)	0.550 (0.112)	0.142 (0.027)
$S1$	51.70 (2.68)	0.279 (0.051)	0.198 (0.030)	0.168 (0.021)
$S2$	53.31 (6.73)	0.435 (0.054)	0.211 (0.016)	0.225 (0.016)
Signification level of the effects ($Pr > F$)				
Treatment	0.6763	<0.0001	<0.0001	<0.0001
Dose (treat.)	0.4296	<0.0001	0.0184	0.0009
R^2 corrected	0.109	0.945	0.861	0.824

In contrast, results clearly show the effect of both factors on absorbance in the three bands of the IR spectrum, with significance levels lower than 0.05 in all cases (usually lower than 0.0001). Moreover, the effect of the treatment is greater than the effect of the dose in all the cases.

As expected, P samples (paraffin + silicone) showed a considerable increment in absorbance at 2,916 cm^{-1} (C–H bonds), while S samples (silicone) present bigger intensities in the band at 1,010 cm^{-1} (Si–O bonds). The band at 2,963 cm^{-1} shows greater absorbances for the "S" samples than for the "P" ones, although the differences are smaller than in the other bands. In all cases, absorbances increase with the dose applied (Fig. 2).

An important aspect is the variability observed among measurements taken from the same stopper. This is a consequence of the lack of homogeneity in the application of the treatment (Fig. 3). It is also important to highlight that on the stopper surface, there are areas where accumulations of the treatment substance appear and display higher absorbances than the rest of the observations on the same stopper. The presence of these accumulations has been visually verified on the stopper surface, coinciding with absorbance values much higher than the average (i.e., absorbance at 1,010 cm^{-1} in Fig. 3a). In spite of this, mean absorbances show significant differences for the different doses. T-test rejects the null hypothesis of equality (at the 95% confidence level) between samples $S1$ and $S2$ for absorbance at 1,010 cm^{-1} and between samples $P1$ and $P2$ for absorbance at 2,916 cm^{-1}.

Discriminant analysis

Two discriminant analyses were made to deduce the treatment type and dose from the spectrometric data. First considers the individual values of the absorbances for the three wavelengths measured (model 1, 125 observations). Second considers the mean values of the same variables for each stopper (model 2, 25 observations). Table 3 shows that both models account for more than 99% of the original variance with two axes.
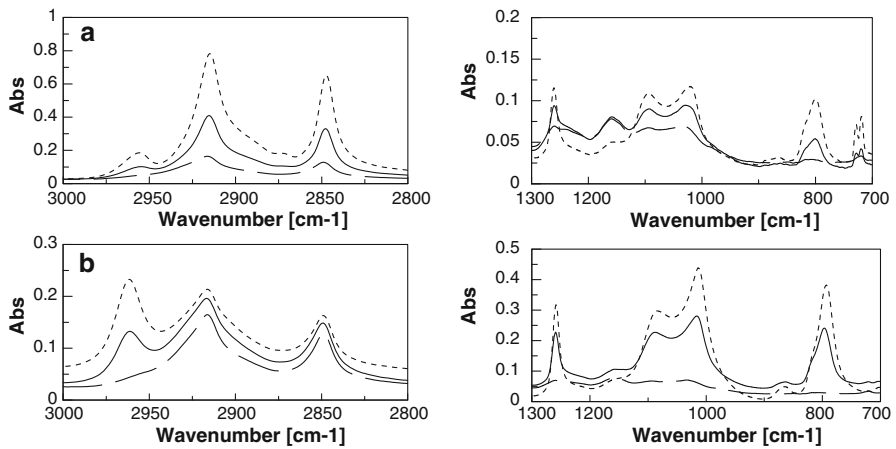
Fig. 2 Dose influence in the considered bands' absorbance (to highlight differences, scales have been adjusted to absorbances in each spectral range). **a** P treatment (paraffin and silicone); **b** S treatment (silicone). Doses: *None* (*0*) (*spaced lines*); low (*P1/S1*) (*solid lines*); high (*P2/S2*) (*dashes*)
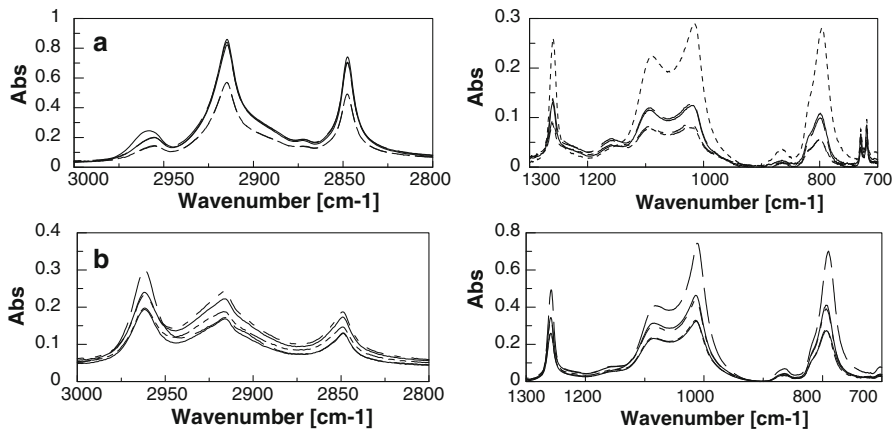

Fig. 3 Treatment variability in the stopper surface: differences in bands among the five spectra from the same stopper. **a** Treatment P2 (paraffin and silicon, 25 mg); **b** Treatment S2 (silicone, 15 mg). To highlight differences, scales have been adjusted to absorbances in each spectral range

The model for the mean values per stopper correctly classifies (treatment and dose) all stoppers but one (96% success rate). The model for the individual observations obtained a higher number of misclassifications (91.2% success rate). As shown in Fig. 4 and Table 4, all misclassifications of individual observations occur at the dose level and none at the treatment level. The same happened for the single mean value misclassified. It is quite probable that all the misclassifications correspond to doses different from those planned. In other words, misclassification may be due to the heterogeneity of the treatment product distribution and not to errors from the ATR-FTIR measurements.

Table 3 Discriminant analysis results to determine the treatment and dose from spectrometric data	Model 1: individual values ($n = 125$)	Model 2: stopper mean values ($n = 25$)
% Accumulated variance		
Axis 1	0.8245	0.8660
Axis 2	0.9926	0.9958
Axis 3	1.0000	1.0000
Crossed validation		
# of misclassified	11	1
% successes	91.2	96.0
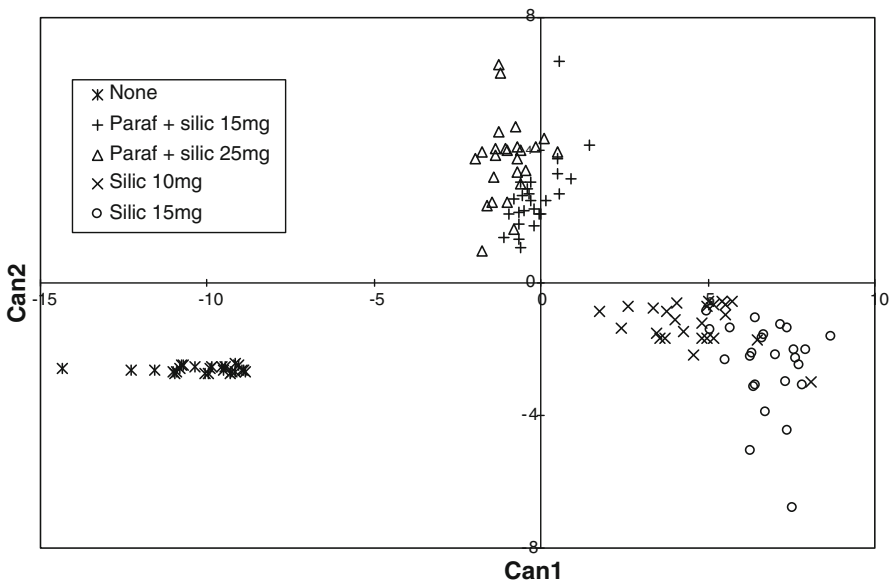
Fig. 4 Discriminant analysis results: plot of individual observations ($n = 125$) on the main two canonical axes (99.26% accumulated variance)

Results suggest that the FTIR technique allows an estimation of the homogeneity of the treatment distribution on the stopper surface. To study it, the variance homogeneity test for the individual measures between the different doses is carried out, using a logarithm transformation (Anderson and McLean 1974). For each treatment, the following variable with the higher discriminant capacity is used: abs2916 for "P" samples and abs1010 for "S" ones (Table 5). As may be seen, increasing the dose for treatment "S" causes a slight increment in variability or a more irregular distribution of the product ($P < 0.05$). In contrast, treatment "P" homogeneity is not affected by an increase in the dose.

Table 4 Cross-validation results for the discriminant model built from individual observations ($n = 125$)

	0	P1	P2	S1	S2	Total
0	25	0	0	0	0	25
P1	0	24	1	0	0	25
P2	0	5	20	0	0	25
S1	0	0	0	23	2	25
S2	0	0	0	3	22	25
Total	25	29	21	26	24	125

Table 5 Equality analysis results for standard deviations among treatment doses

	Treatment "P" (paraffin and silicone)		Treatment "S" (only silicone)	
	abs2916		abs1010	
	P1	P2	S1	S2
Count	25	25	25	25
Average	0.416	0.550	0.279	0.435
Standard deviation	0.104	0.143	0.072	0.115
Variance of standard deviation	0.011	0.020	0.005	0.013
F test to compare standard deviations				
F	0.52		5.55	
P value	0.490		0.046	

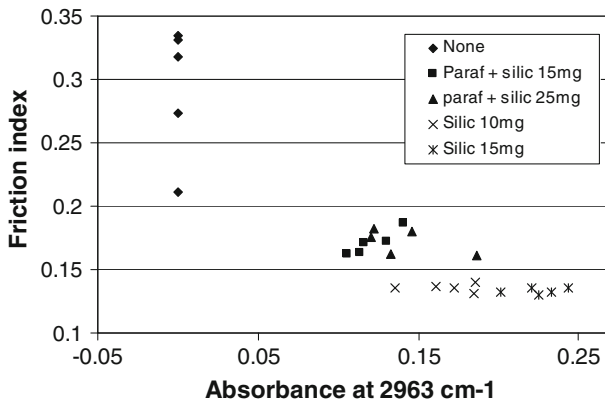In each case, the variable showing higher discriminant power is analyzed

Fig. 5 Effect of treatment type and dose (measured in terms of absorbance at 2,963 cm^{-1}) on friction behavior

Friction index

Relationships between spectrometric data and friction behavior for each stopper have also been studied; Fig. 5 shows the case of one of the selected bands (at 2,963 cm^{-1}). As expected, the friction index is affected by treatment type, but the dose effect is practically imperceptible (ANOVA results not shown). Stoppers without treatment ("00" samples) show a friction index larger than 0.2; those treated with paraffin and silicone ("P" samples), between 0.15 and 0.2; and those with silicone only ("S" samples), less than 0.15. The chart also shows the treatment effect over the variability (dispersion) of this parameter: larger in the "00" stoppers, reduced in the "P" ones, and practically non-existent for the "S".

   These data show the possibility of reducing the variability in the mechanical behavior of a stopper lot based on an adequate control of the surface treatment. Results suggest the possibility that the spectrometric data may be used to predict the efficacy of the surface treatment in relation to the friction index. Different regression models have been developed using this index as a dependent variable and absorbances, their logarithms, and their inverses as independent variables. The model shown in Table 6 is obtained by applying a stepwise regression. The good results obtained for the fit (friction index) reflect the close relationship between surface treatment and friction behavior (Fig. 6). The spectra absorbance changes

Table 6 Regression model to estimate the friction index from spectrometric data

Parameter	Estimate	Standard error	T statistic	P value
CONSTANT	0.126575	0.00775223	163.276	0
abs1010av	−0.0340745	0.0138342	−246.306	0.0255
abs2916av	0.205864	0.0328313	627.035	0
1/LOG(abs2916av)	0.0346862	0.00695883	498.449	0.0001

R-squared (adjusted for df) = 92.96%
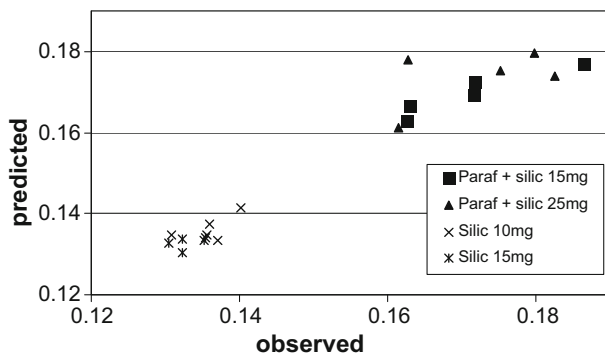
Standard Error of Est. = 0.005

Fig. 6 Observed vs. estimated values for friction index according to regression model (Table 6)

(which are a consequence of variations in the amount of surface treatment coating) imply changes in friction for the same kind of treatment and dose.

Conclusion

Results show the ATR-FTIR spectroscopy capacity to determine the type and dose of surface treatment applied on the stopper. This non-destructive technique is therefore a valuable tool to improve stopper quality control, as the traditional techniques based on extraction with solvents (DCM) are not useful for this purpose.

Due to the variability in the distribution of the surface treatment, it is necessary to take several measurements to correctly determine the dose applied. Using spectra obtained in small areas (2 mm^2), the treatment quality, in terms of uniformity of the layer coating each stopper, can be estimated.

For the most common surface treatments, consisting mainly of silicone and paraffin, the absorbance at the three selected wavelengths (1,010, 2,916, and $2,963 \text{ cm}^{-1}$) allows:

(a) the stoppers to be classified by type and dose of treatment applied,
(b) the homogeneity of the distribution of the product to be evaluated, and,
(c) the surface treatment effect on the friction performance of the stopper to be predicted.

References

Anderson VL, McLean RA (1974) Design of experiments. A realistic approach, Marcel Dekker Inc., New York

Bradley E, Castle L (2003) Investigation of the migration of chemicals from agglomerate, plastic and natural cork stoppers. Report FD 02/27 Food Standards Agency, York, England

Canals T, Riba JR, Cantero R, Cansino J, Domingo D, Iturriaga H (2008) Characterization of paper finishes by use of infrared spectroscopy in combination with canonical variate analysis. Talanta 77(2):751–757

Chatonnet P, Labadie D (2003) Control of the stoppers conformity: objectives and parameters for professionals. Rev Fr d 'Oenol 198:20–29

Fortes MA, Rosa ME, Pereira H (2004) Cork. IST Press, Lisboa, Portugal

Giunchi A, Versari A, Parpinello GP, Galassi S (2008) Analysis of mechanical properties of cork stoppers and synthetic closures used for wine bottling. J Food Eng 88(4):576–580

Gonzalez-Adrados JR, Gonzalez-Hernandez F, De Ceca JLG, Caceres-Esteban MJ, Garcia-Vallejo MC (2008) Cork-wine interaction studies: Liquid absorption and non-volatile compound migration. Journal International Des Sciences De La Vigne Et Du Vin 42(3):163–168

Kontoudakis N, Biosca P, Canals R, Fort F, Canals JM, Zamora F (2008) Impact of stopper type on oxygen ingress during wine bottling when using an inert gas cover. Aust J Grape Wine Res 14:116–122

Lopes P, Saucier C, Teissedre PL, Glories Y (2007) Main routes of oxygen ingress through different closures into wine bottles. J Agric Food Chem 55(13):5167–5170

Ortega-Fernandez C, Gonzalez-Adrados JR, Garcia-Vallejo MC, Calvo-Haro R, Caceres-Esteban MJ (2006) Characterization of surface treatments of cork stoppers by FTIR-ATR. J Agric Food Chem 54(14):4932–4936

Pereira H (2007) Cork: Biology. Production and Uses. Elsevier, Oxford, UK

Riboulet JM, Alegoët C (1986) Practical aspects of wine corkage. Bourgogne Publications, Chaintré, France

Six T, Feigenbaum A (2003) Mechanism of migration from agglomerated cork stoppers. Part 2: Safety assessment criteria of agglomerated cork stoppers for champagne wine cork producers, for users and for control laboratories. Food-Additives-and-Contaminants 20(10):960–971

Six T, Feigenbaum A, Riquet A-M (2002) Mechanism of Migration from Agglomerated Cork Stoppers: I. An Electron Spin Resonance Investigation. J Appl Polym Sci 83:2644–2654

Skouroumounis GK, Kwiatkowski MJ, Francis IL, Oakey H, Capone DL, Duncan B et al (2005) The impact of closure type and storage conditions on the composition, colour and flavour properties of a Riesling and a wooded Chardonnay wine during five years' storage. Aust J Grape Wine Res 11(3):369–384

Yang P, Meng XF, Zhang ZY, Jing BX, Yuan J, Yang WT (2005) Thickness measurement of nanoscale polymer layer on polymer substrates by attenuated total reflection infrared spectroscopy. Anal Chem 77(4):1068–1074